Supporting Information

Heterostructure Construction of Covalent Organic Framework/Ti_3C_2-MXene for High-efficiency Electrocatalytic CO_2 Reduction

Liyuan Zhou,[a] Qingyong Tian,[a] Xiaoqing Shang,[a] Yanming Zhao,[a] Weijing Yao,[b] Hongpo Liu,[a] Qun Xu [a*]*

Supplementary Text

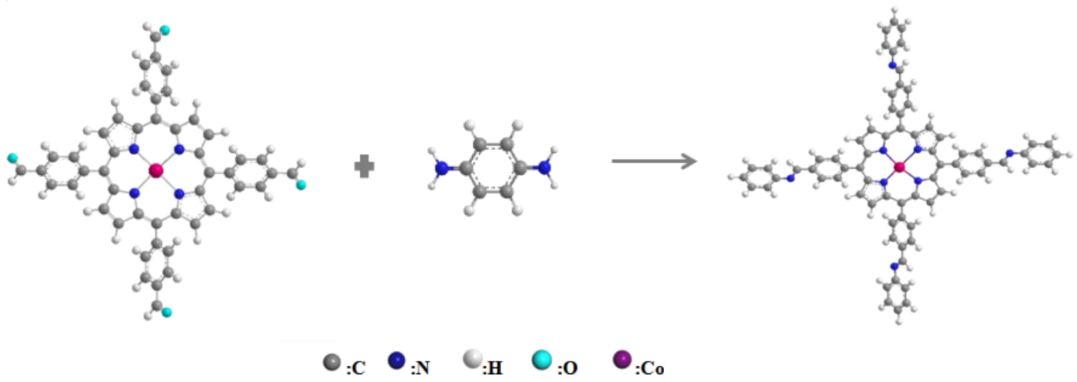

Figure S1. Synthetic route diagram of Por-COF-Co with the reaction solvent of 1, 2- dichlorobenzene、butanol and 6M acetic acid and reaction conditions of 120 °C for three days.

*To whom correspondence should be addressed. Tel: +86-27-63886819. E-mail: tianqy@zzu.edu.cn (Q. Tian) and qunxu@zzu.edu.cn (Q. Xu).

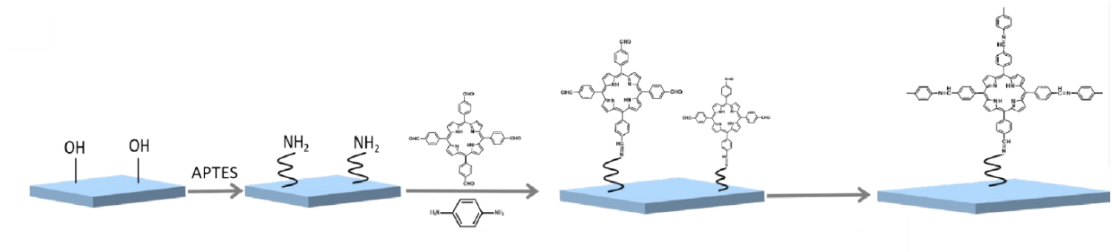

Figure S2. Schematic diagram of in-situ growth of COF on the surface of MXene nanosheets using Schiff base condensation polymerization method.

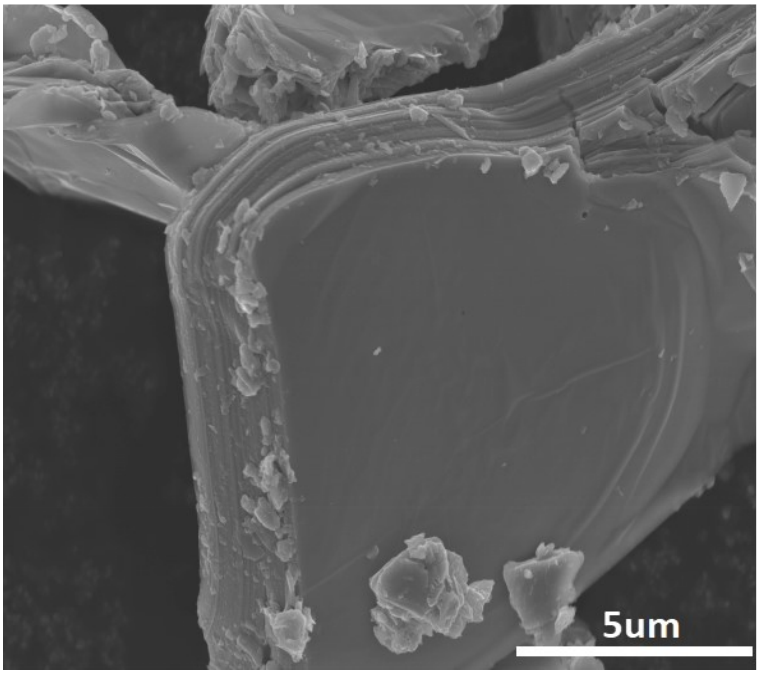

Figure S3. SEM images of Ti_3C_2 MXene nanosheets.

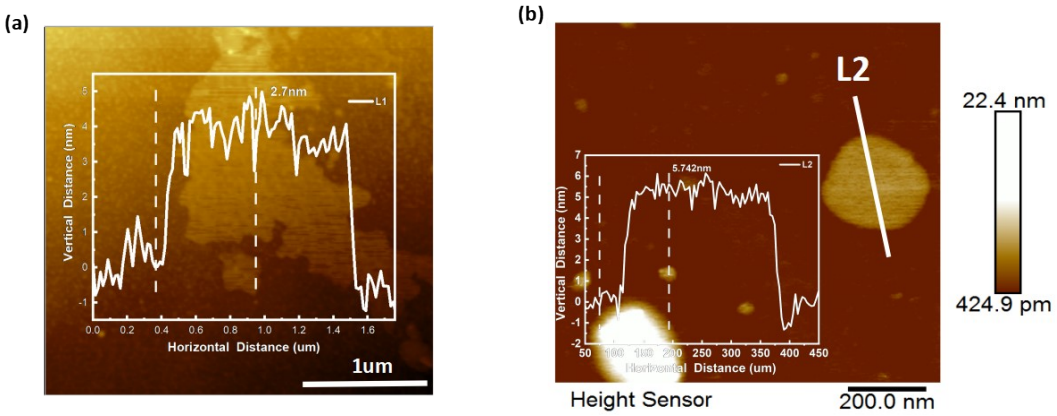

Figure S4. AFM image with the measured thickness of (a) Ti_3C_2 MXene nanosheets, (b) Por-COF.

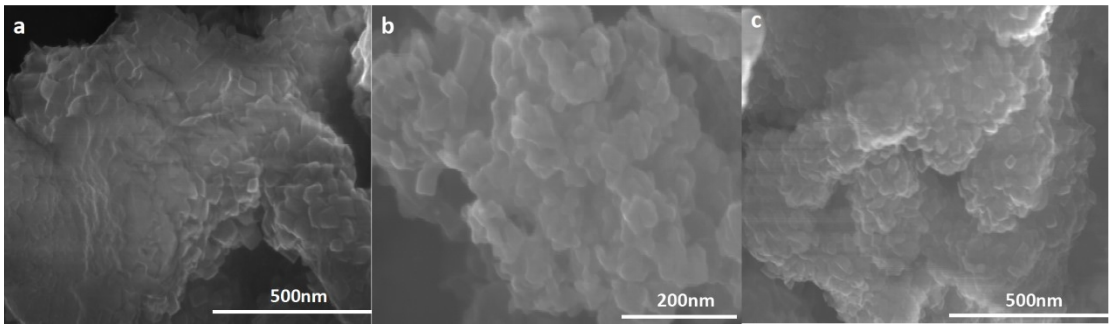

Figure S5. SEM images of (a) MXene@Por-COF-Co-3 heterostructure, (b) MXene@Por-COF-Co-5 heterostructure, (c) MXene@Por-COF-Co-7 heterostructure.

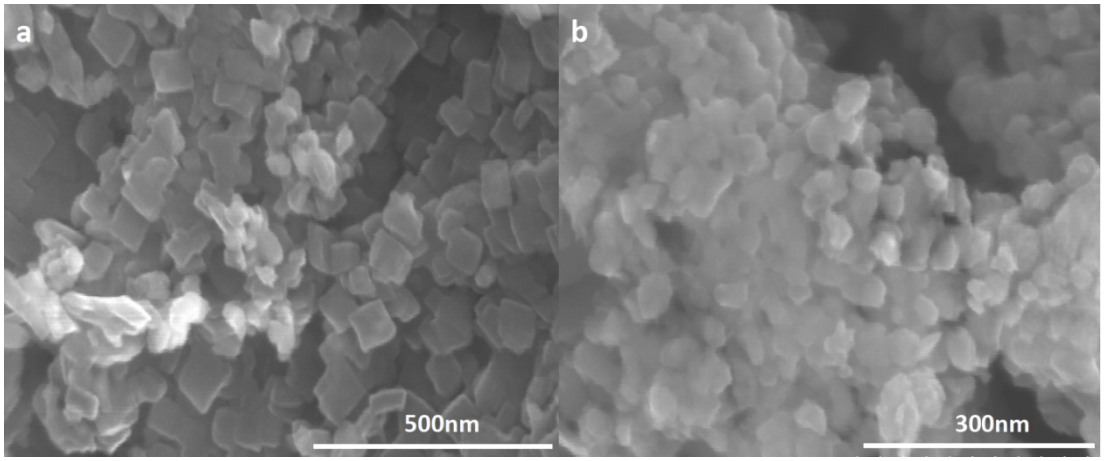

Figure S6. SEM images of (a) MXene@Por-COF-3 heterostructure, (b) MXene@Por-COF-5 heterostructure.

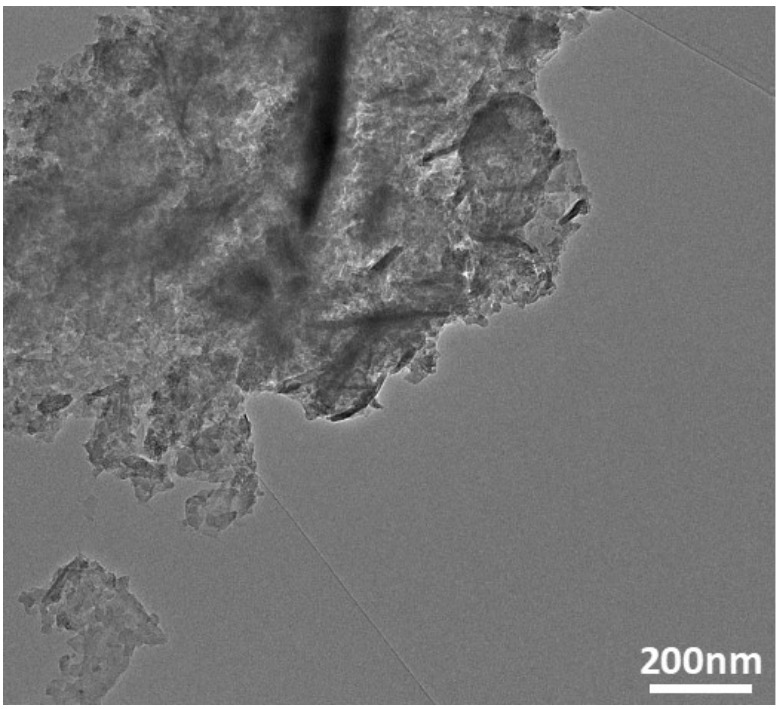

Figure S7. TEM images of MXene@Por-COF-Co-7 heterostructure.

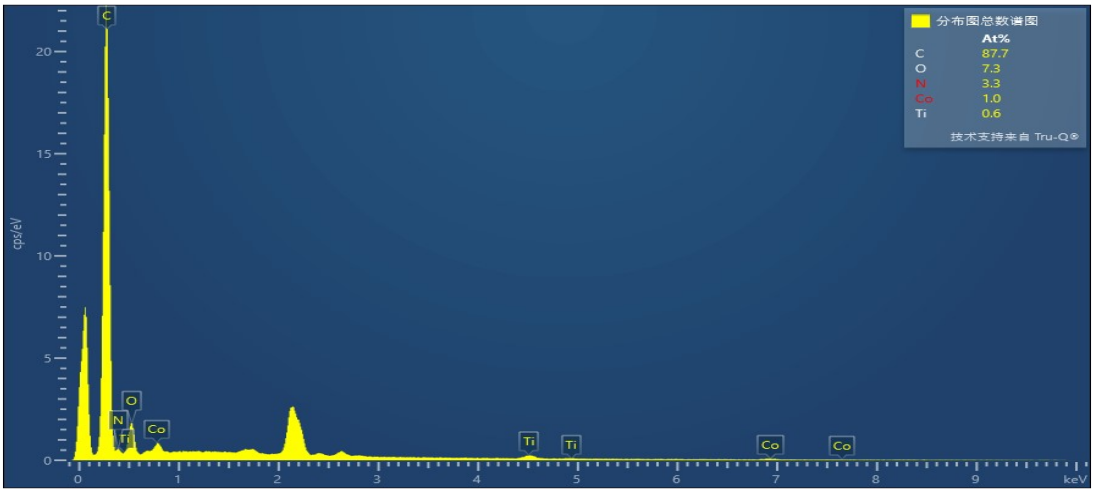

Figure S8. The EDS image of MXene@Por-COF-Co-7.

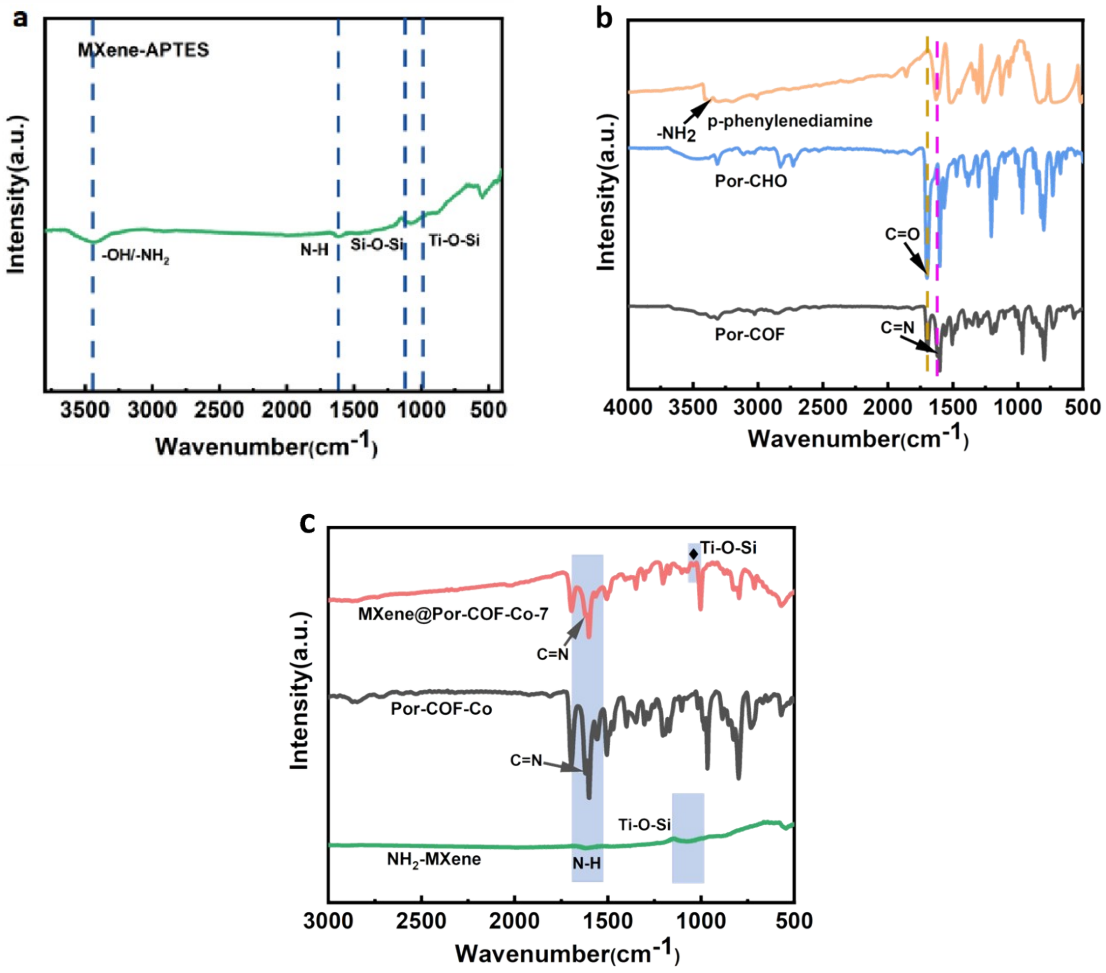

Figure S9. FTIR spectra of the (a) amino-functionalized Ti_3C_2 MXene, (b) Por-COF compared with reactants of Por-CHO and p-phenylenediamine，(c) MXene@Por-COF-Co-7 compared with reactants of Por-COF-Co and NH_2-MXene.

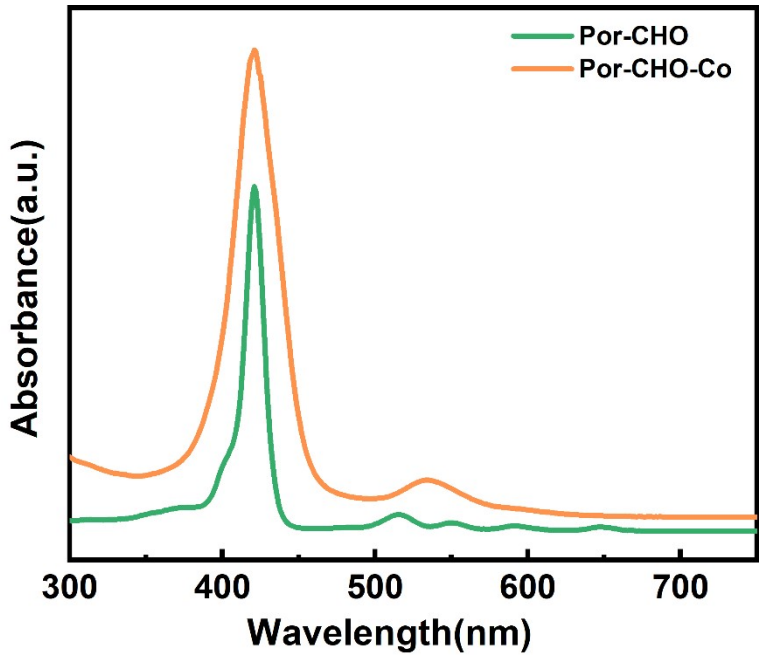

Figure S10. UV-vis spectra of Por- CHO, Por-CHO-Co.

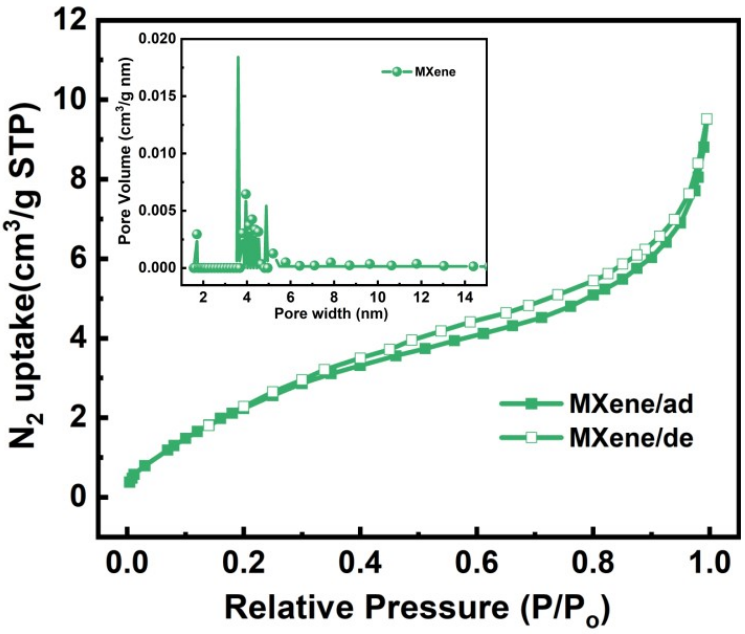

Figure S11. N_2 sorption isotherms of MXene at 77 K (inset pore-size distribution profile). The N_2 sorption revealed that MXene has Brunauer-Emmer Teller (BET) surface area 10.5771 m^2g^{-1}.

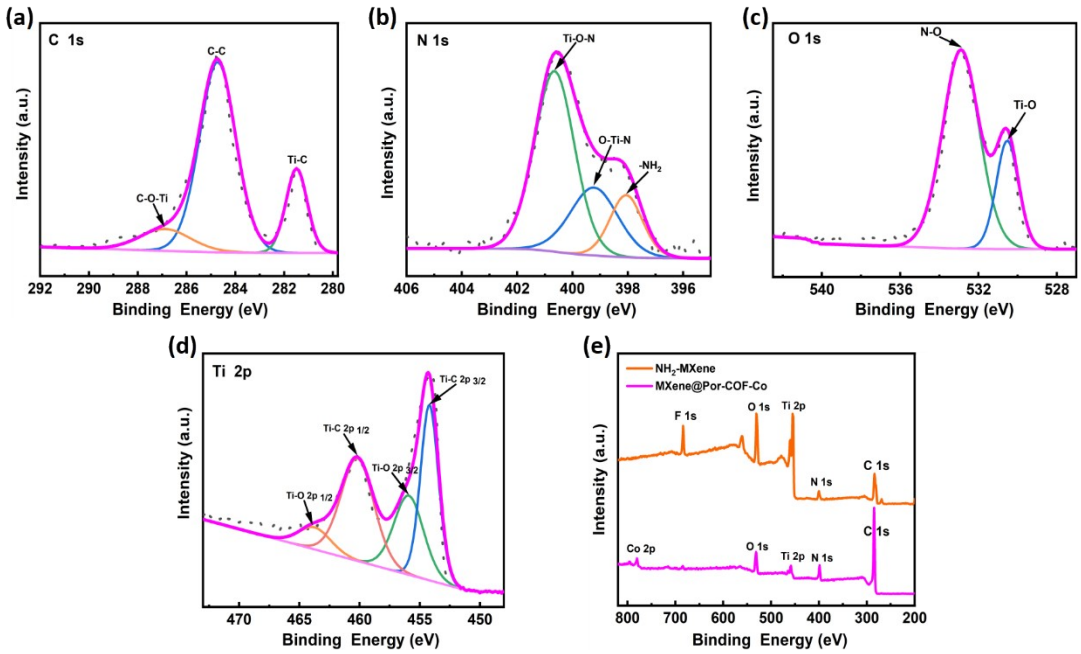

Figure S12. The XPS (a) C 1s, (b) N 1s, (c) O 1s and (d) Ti 2p spectra of the NH_2-MXene; (e) XPS spectra of NH_2-MXene and MXene@Por-COF-Co-7 heterostructure.

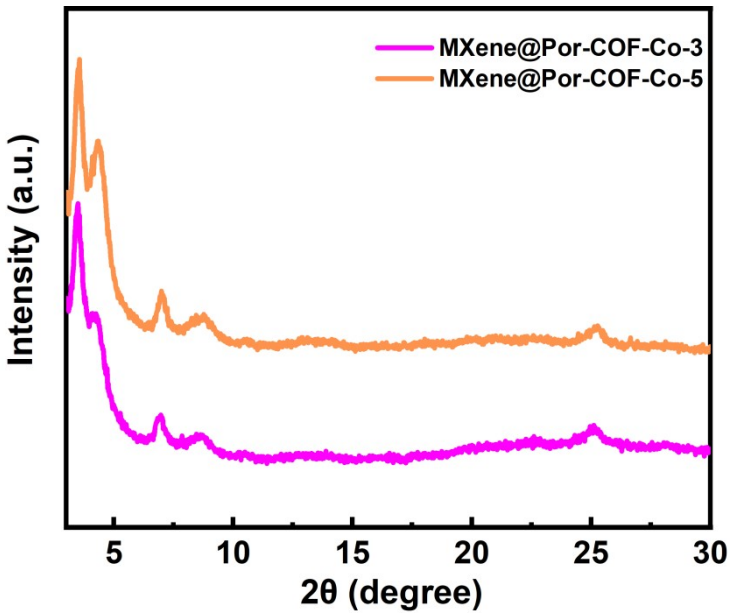

Figure S13. PXRD patterns of MXene@Por-COF-Co-3 and MXene@Por-COF-Co-5.

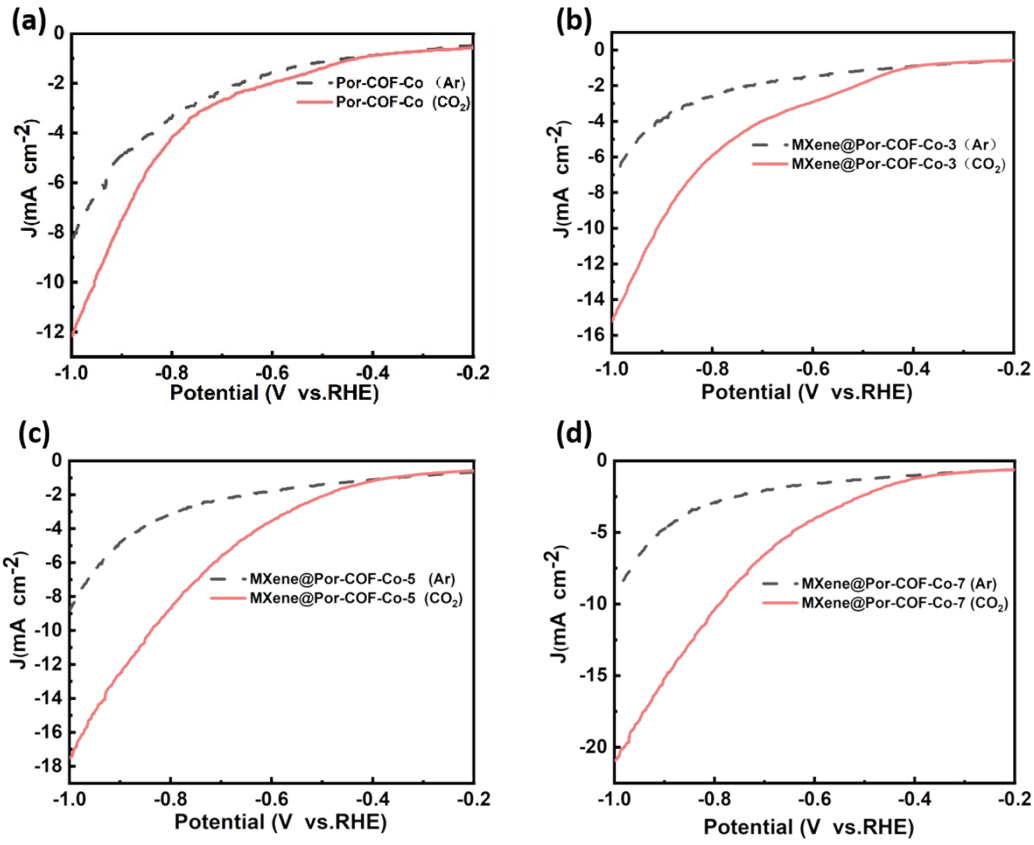

Figure S14. LSV curve in the Ar-saturated and CO_2-saturated 0.5 M $KHCO_3$ electrolyte at a scan rate of 10 mV s^{-1} for (a) Por-COF-Co, (b) MXene@Por-COF-Co-3, (c) MXene@Por-COF-Co-5, (d) MXene@Por-COF-Co-7.

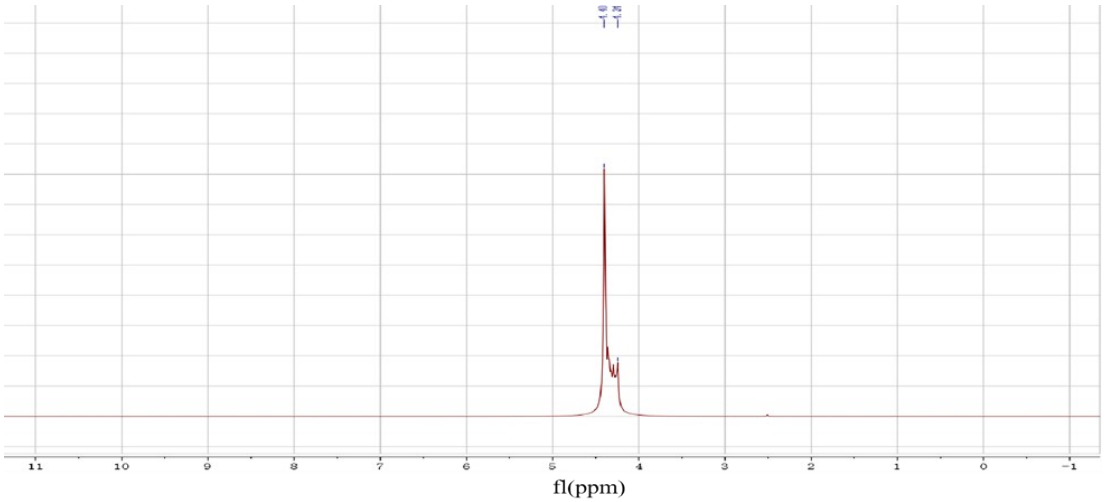

Figure S15. ^{1}H NMR spectra of MXene@Por-COF-Co for the electrolyte test after CO_2RR in CO_2-saturated 0.5 M $KHCO_3$.

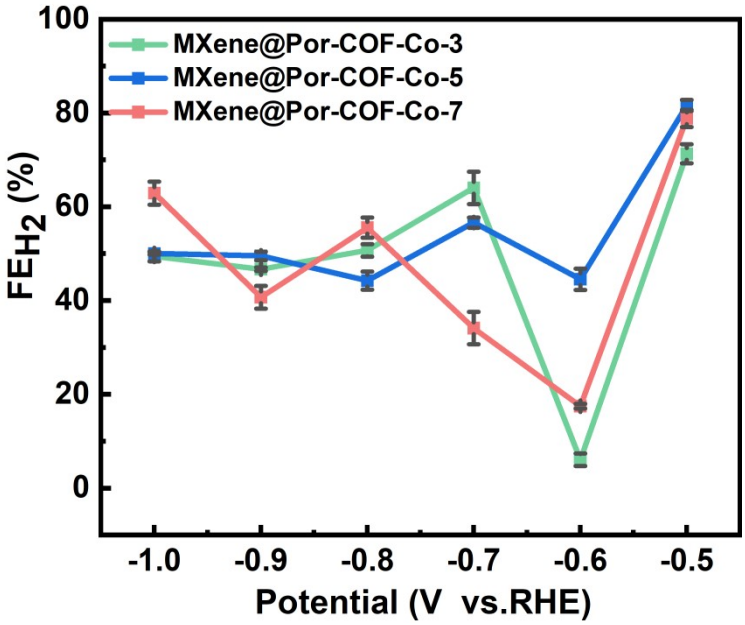

Figure S16. FE_{H2} from -0.5 to -1 V vs RHE of MXene@Por-COF-Co-3, MXene@Por-COF-Co-5 and MXene@Por-COF-Co-7.

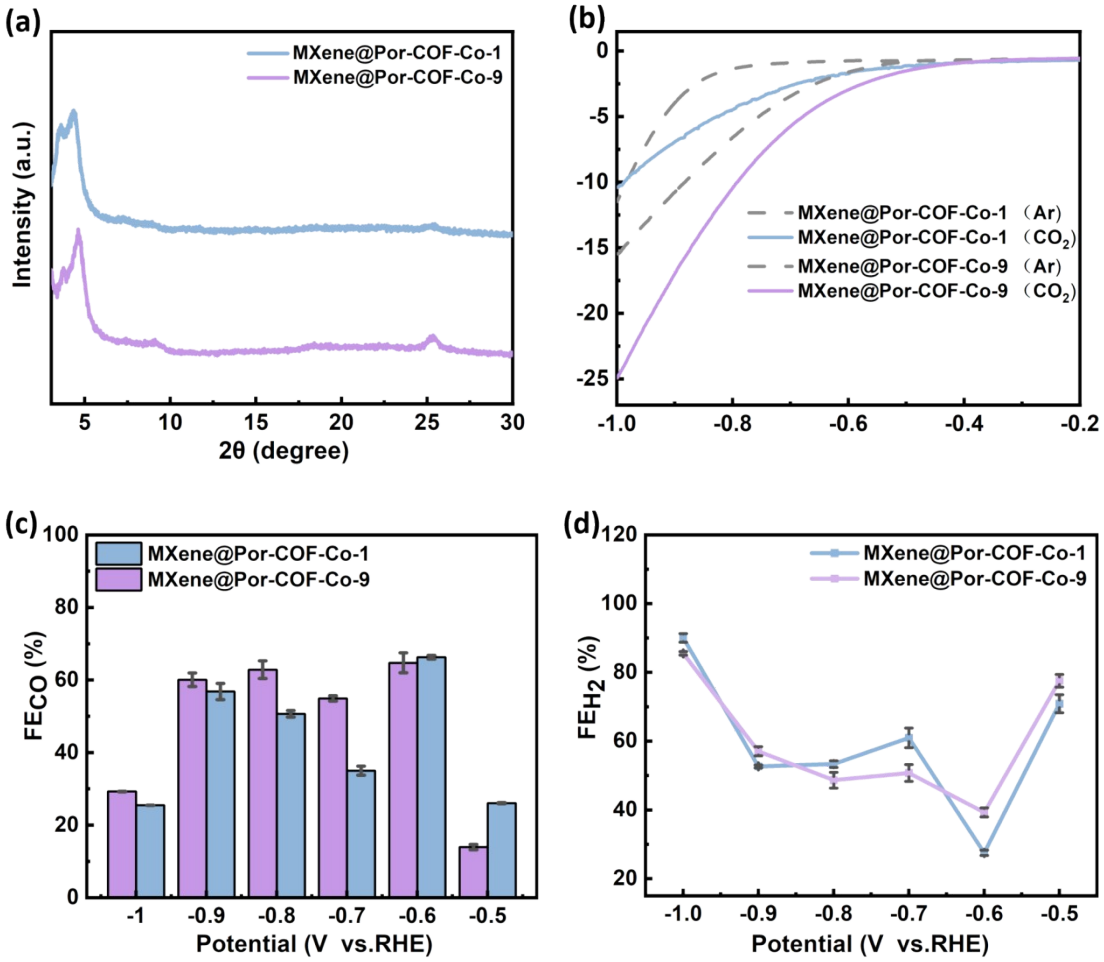

Figure S17. (a) PXRD patterns of MXene@Por-COF-Co-1、MXene@Por-COF-Co-9. (b) LSV curve in the Ar-saturated and CO_2-saturated 0.5 M $KHCO_3$ electrolyte at a scan rate of 10 mV s^{-1} for MXene@Por-COF-Co-1 and MXene@Por-COF-Co-9. (c) The FE_{CO} calculated potential ranges from -0.5 to - 1.0 V, (d) FE_{H2} from -0.5 to -1 V vs RHE of MXene@Por-COF-Co-1 and MXene@Por-COF-Co-9.

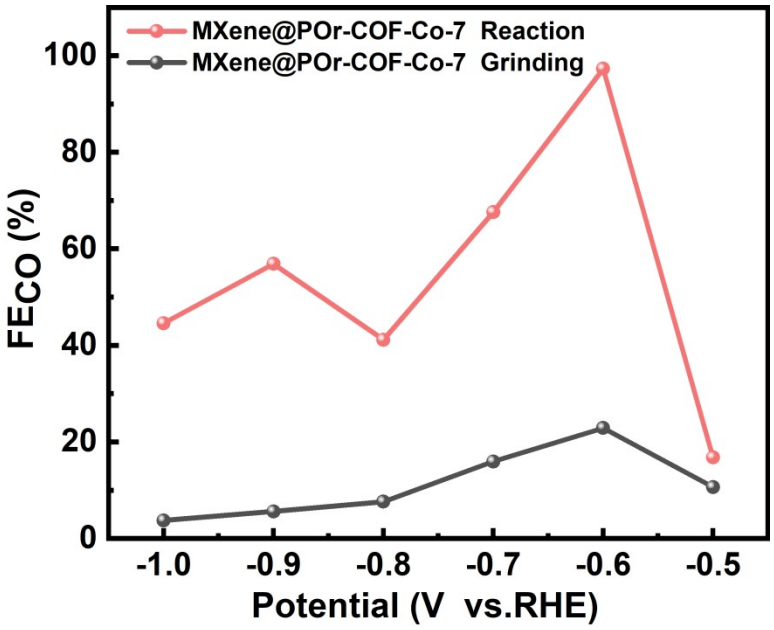

Figure S18. The FE_{CO} from −0.5 to −1 V vs RHE of MXene@Por-COF-Co-7 and physical mixing NH_2-MXene/Por-COF-Co.

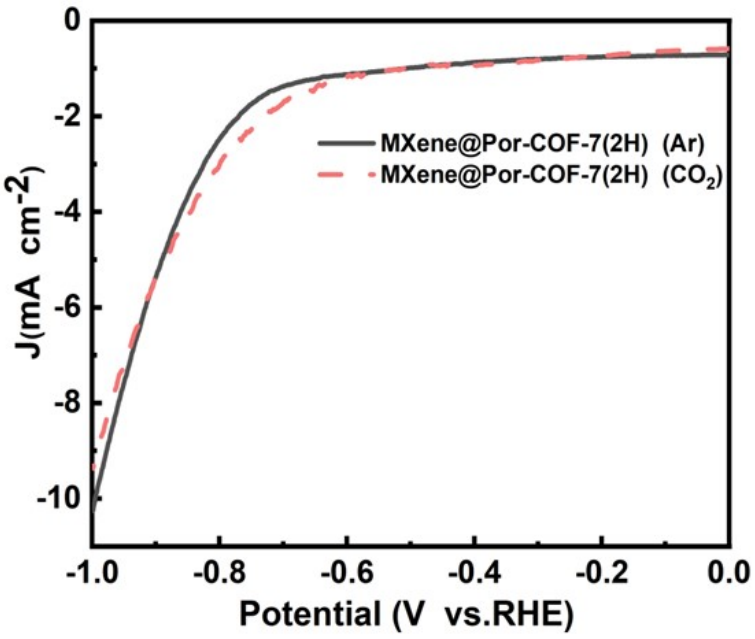

Figure S19. LSV curve in the Ar-saturated and CO_2-saturated 0.5 M $KHCO_3$ electrolyte at a scan rate of 10 mV s^{-1} for MXene@Por-COF(2H).

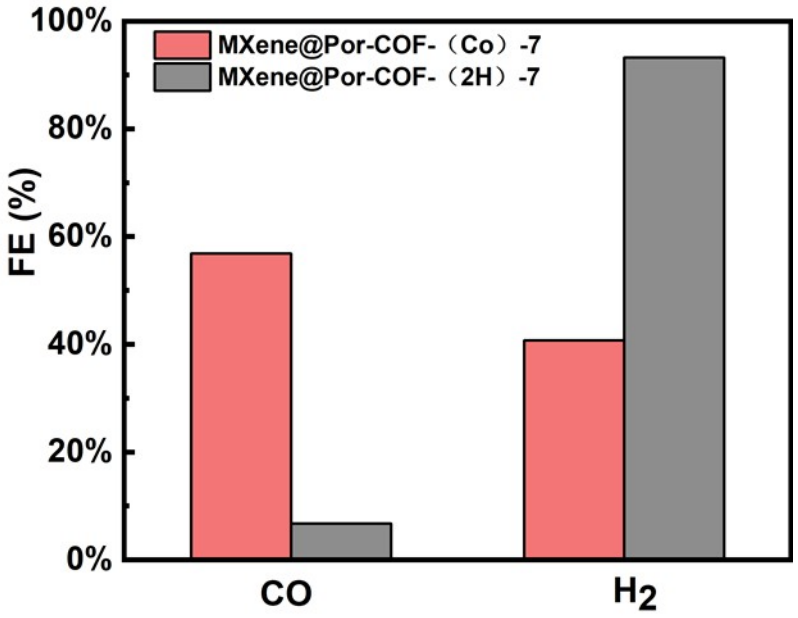

Figure S20. The selectivity and activity of the MXene@Por-COF-Co-7 and MXene@Por-COF(2H) were compared at -0.9 V vs. RHE using identical conditions.

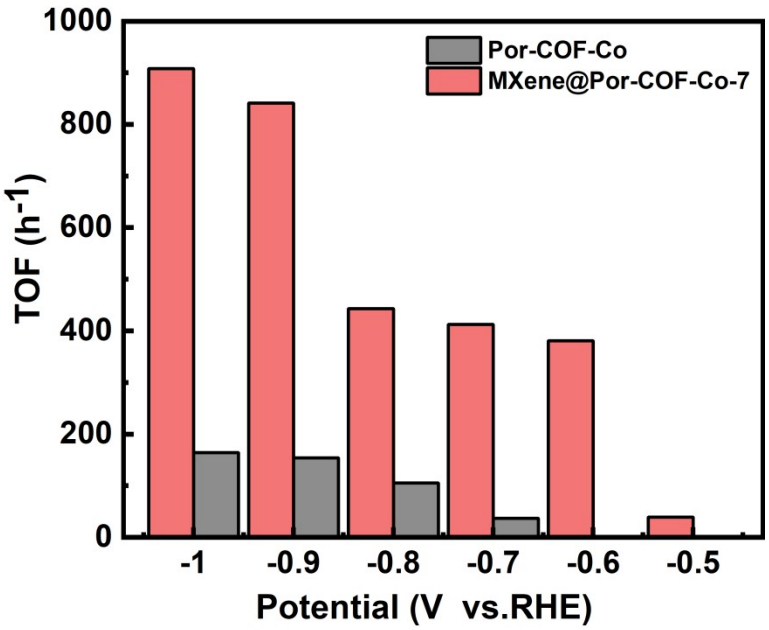

Figure S21. TOF (h^{-1}) at different potentials for Por-COF-Co and MXene@Por-COF-Co-7.

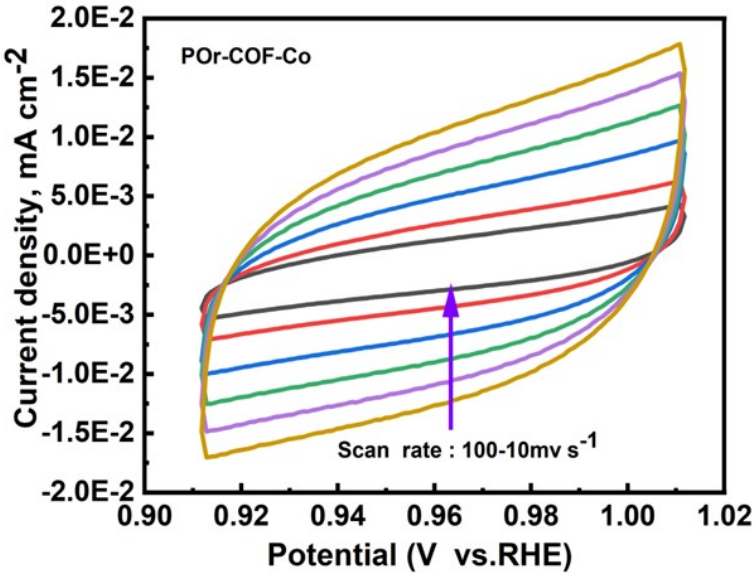

Figure S22. Cyclic voltammertrys (CV) curves of Por-COF-Co in the region of 0.91 ~ 1.01 V vs. RHE at various scan rate (10 ~ 100 mV s^{-1}).

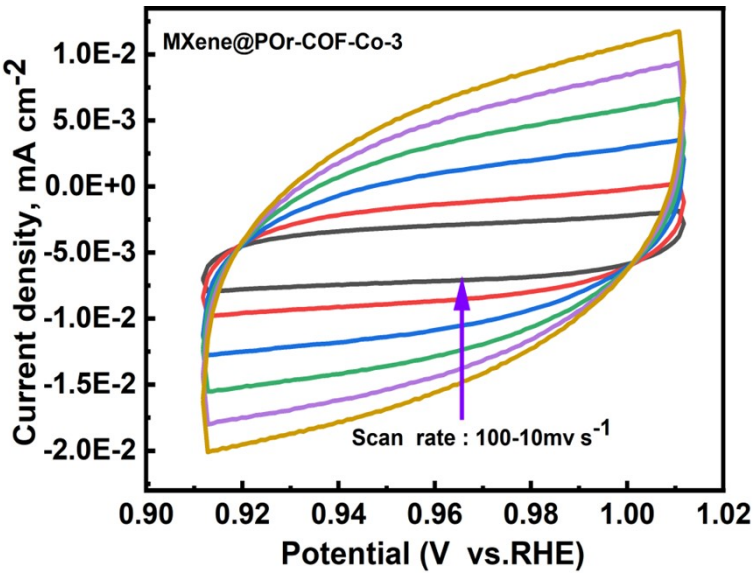

Figure S23. Cyclic voltammertrys (CV) curves of MXene@Por-COF-Co-3 in the region of 0.91 ~ 1.01 V vs. RHE at various scan rate (10 ~ 100 mV s^{-1}).

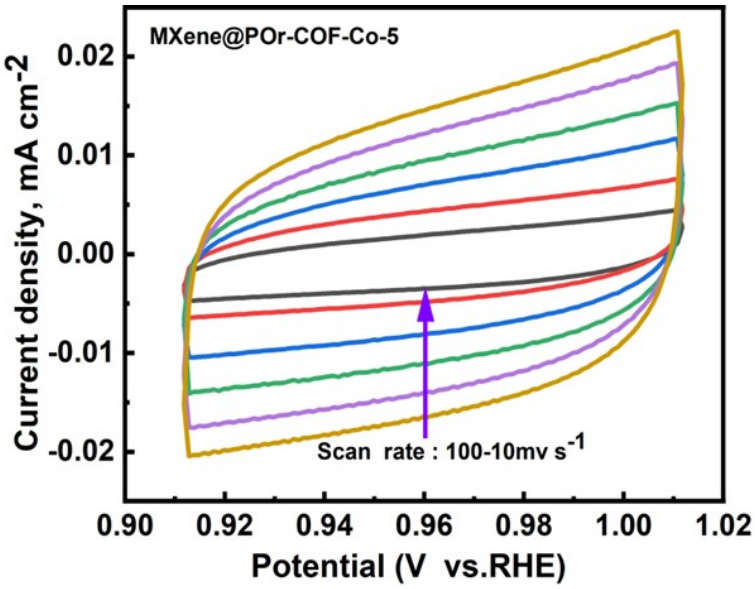

Figure S24. Cyclic voltammertrys (CV) curves of MXene@Por-COF-Co-5 in the region of 0.91 ~ 1.01 V vs. RHE at various scan rate (10 ~ 100 mV s^{-1}).

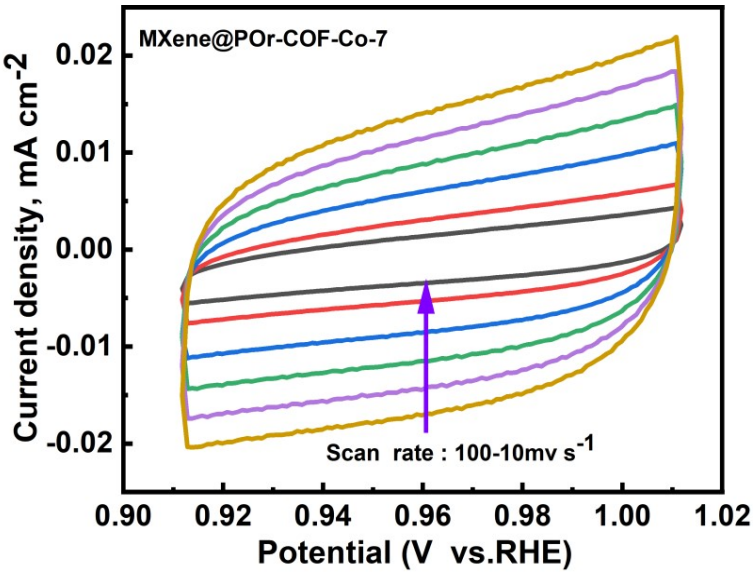

Figure S25. Cyclic voltammertrys (CV) curves of MXene@Por-COF-Co-7 in the region of 0.91 ~ 1.01 V vs. RHE at various scan rate (10 ~ 100 mV s^{-1}).

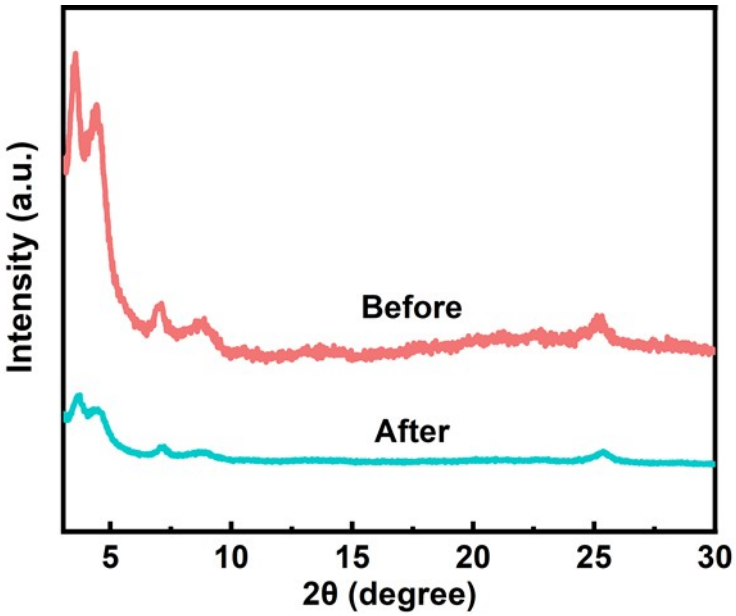

Figure S26. The XRD patterns before and after electrocatalytic CO_2RR reaction of MXene@Por-COF-Co-7.

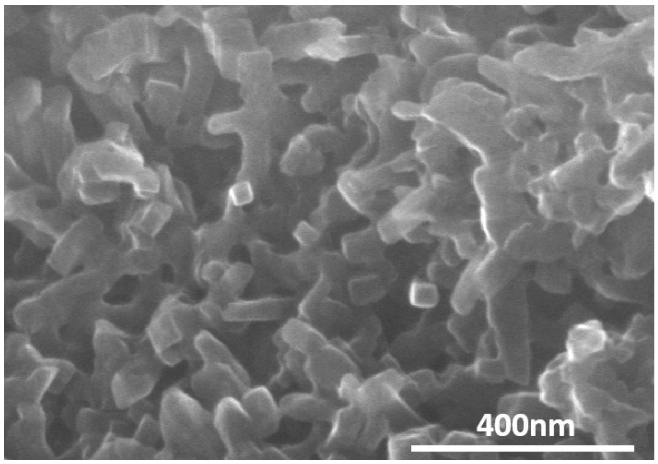

Figure S27.The SEM images of MXene@Por-COF-Co-7 after electrocatalytic CO_2RR reaction.

Table S1. Comparison of catalyst with other reported high efficiency CO-selective CO_2 reduction electrocatalysts

Catalyst	Electrolyte	Applied Potential (V vs RHE)	Faradaic efficiency of CO (%)	Reference
MXene@Por-COF-Co-7	**0.5 M $KHCO_3$**	**-0.6**	**97.28**	**This work**
COF-366-Co	0.5 M $KHCO_3$	-0.56	~72	1
COF-367-Co	0.5 M $KHCO_3$	-0.56	~68	1
TTF-Por(Co)-COF	0.5 M $KHCO_3$	-0.6	90	2
CoPc-PDQ-COF	0.5 M $KHCO_3$	-0.6	85	3
COF-300-AR	0.1 M $KHCO_3$	-0.7	53	4
COF-366-$(OMe)_2$-Co@CNT	0.5 M $KHCO_3$	-0.58	~92	5
Co-PMOF	0.5 M $KHCO_3$	-0.6	~70	6
CoFPc	0.5M $NaHCO_3$	-0.6	86	7
TCPP(Co)/Zr-BTB	0.5 M $KHCO_3$	-0.6	~60	8
Co@Pc/C	0.5 M $KHCO_3$	-0.6	~70	9
2.5-CoPc/ZIS-180	0.5 M $KHCO_3$	-0.6	20	10

References

1 S. Lin, C. S. Diercks, Y. B. Zhang, N. Kornienko, E. M. Nichols, Y. B. Zhao, A. R. Paris, D. Kim, P. Yang, O. M. Yaghi and C. J. Chang, Science, 2015, 349, 1208-1213

2 Q. Wu, R. K. Xie, M. J. Mao, G. L. Chai, J. D. Yi, S. S. Zhao, Y. B. Huang and R. Cao, ACS Energy, 2020, 5, 1005-1012.

3 N. Huang, K. H. Lee, Y. Yue, X. Y. Xu, S. Irle, Q. H. Jiang and D. L. Jiang, Angew. Chem.,Int. Ed., 2020, 59, 16587-16593.

4 H. Y. Liu, J. Chu, Z. L. Yin, X. Cai, L. Zhuang and H. X. Deng, Chem, 2018, 4, 1696-1709.

5 Y. Lu, J. Zhang, W. B. Wei, D. D. Ma, X. T. Wu and Q. L. Zhu, ACS Appl. Mater. Interfaces, 2020, 12, 37986-37992.

6 Y. R. Wang, Q. Huang, C. T. He, Y. F. Chen, J. Liu, F. C. Shen and Y. Q. Lan, Nat. Commun., 2018, 9, 8.

7 N. Morlanés, K. Takanabe and V. Rodionov, ACS Catal., 2016, 6, 3092-3095.

8 X. D. Zhang, S. Z. Hou, J. X. Wu and Z. Y. Gu, Chem.-Eur. J., 2020, 26, 1604-1611.

9 C. He, Y. Zhang, Y. F. Zhang, L. Zhao, L. P. Yuan, J. N. Zhang, J. M. Ma and J. S. Hu, Angew. Chem.,Int. Ed., 2020, 59, 4914-4919.

10 C. J. Chen, X. F. Sun, D. X. Yang, L. Lu, H. H. Wu, L. R. Zheng, P. F. An, J. Zhang and B. X. Han, Chem. Sci., 2019, 10, 1659-1663.